Dynamic response on a nanometer scale of binary phospholipid-cholesterol vesicles: Low-frequency Raman scattering insight

N. V. Surovtsev* and S. V. Adichtchev
Institute of Automation and Electrometry, Russian Academy of Sciences, Novosibirsk 630090, Russia

(Received 16 August 2021; accepted 18 October 2021; published 12 November 2021)

Low-frequency Raman spectroscopy was used to study the dynamic response on a nanometer scale of aqueous suspensions of two-component lipid vesicles. Binary mixtures of saturated phospholipid (1,2-dipalmitoyl-sn-glycero-3-phosphocholine, DPPC) and cholesterol are interesting for possible coexistence of solidlike and liquid-ordered phases, while the phase coexistence was not reported for unsaturated phospholipid (1,2-dioleoyl-sn-glycero-3-phosphocholine, DOPC) and cholesterol mixtures. The DOPC-DPPC mixtures represent the well-documented case of coexisting domains of solidlike and liquid-disordered phases. These three series of lipid mixtures are studied here. A broad peak with the maximum in the range of 30–50 cm^{-1} and a narrow peak near 10 cm^{-1} are observed in the Raman susceptibility of the binary mixtures and attributed to the acousticlike vibrational density of states and layer modes, respectively. Parameters of the broad and narrow peaks are sensitive to lateral and conformational hydrocarbon chain ordering. It was also demonstrated that the low-frequency Raman susceptibility of multicomponent lipid bilayers allows one to determine the phase state of lipid bilayers and distinguish the homogeneous distribution of molecular complexes from coexisting domains with sizes above several nanometers. Thus, the low-frequency Raman spectroscopy provides unique information in studying phase coexistence in lipid bilayers.

DOI: 10.1103/PhysRevE.104.054406

I. INTRODUCTION

Lipid bilayers, being models of biological membranes and drug delivery vehicles, are subjects of numerous research studies. Various experimental methods can determine the phase state of lipid bilayers (liquidlike or solidlike for lateral order) and the conformational state of hydrocarbon chains. Structural methods (X-ray or neutron elastic scattering) characterize density distributions across the lipid bilayer and molecule-molecule correlations in the lateral plane [1–5]. There are experimental techniques, which provide information about single-molecule conformations and dynamics in lipid layers (nuclear magnetic resonance [6–8], electron spin resonance [9,10], Raman [11–13], and infrared [11,14] spectroscopy). Some optical techniques (Raman [15] and fluorescence microscopies [16,17]) characterize material with micron resolution and are capable to reveal possible spatial segregation of components. However, the actual problem of component and phase separation in multicomponent lipid bilayers [18,19] needs also experimental information about layer properties on a nanometer scale. There are only a few methods (for example, tip-enhanced Raman scattering [20]), which can be directly applied to the problem of the coexistence of domains of different phases and compositions on the nanometer scale. An alternative is a vibrational spectroscopy for acousticlike excitations with nanometer wavelengths. It can be expected that nanometer inhomogeneities in lipid bilayers should affect vibrational excitations with nanometer wavelengths. This approach should also be applicable for transient inhomogeneities in the lipid bilayer that occur in biological membranes since the THz vibrational spectrum reflects a snapshot of the structure on a scale of picoseconds. Domains of lipids with high lateral mobility but with ordered conformations of hydrocarbon chains referred to as rafts are considered a key factor for various cellular processes [21–26].

THz vibrational response in condensed matter materials reflects acousticlike excitations with nanometer wavelengths. This response can be measured using inelastic neutron and x-ray scattering (INS and IXS). There are several research groups studying the THz vibrational response in oriented phospholipid bilayers with INS and IXS [27–34]. Examples of INS and IXS applications for multicomponent lipid bilayers can be found [30,32]. INS and IXS are labor- and cost-consuming experimental techniques. Low-frequency Raman spectroscopy could be a complementary technique in studying the THz vibrational density of states, having high spectral resolution and availability. The peculiarity of the Raman scattering is the scattering wave-vector selection rule, which forbids the Raman signal from THz acoustic plane waves. However, localized acousticlike modes and propagating acoustic excitations in the case of structural disorder bypass this limitation [33].

Experimental studies of the low-frequency Raman scattering in frozen suspensions of phospholipid vesicles revealed relatively sharp peaks that were attributed to the vibrational eigenmodes modulating the layer thickness [34,35]. Since these vibrational modes involve the movement of at least several nanometers of the lateral surface, they can be applied for the problem of the coexistence of domains of different

*Corresponding author: snv@iae.nsk.su

compositions in multicomponent lipid bilayers. This has been done for some binary [36] and ternary [37] membranes. However, the manifestation of the low-frequency peak in the direct Raman spectrum only for frozen suspensions is a drawback of this approach if the phase diagram of multicomponent membranes is considered at physiological temperatures. The low-frequency Raman susceptibility spectrum of saturated phospholipid vesicles at physiological temperatures was studied in Ref. [38] to overcome this problem. It was found that the low-frequency Raman susceptibility reveals a broad peak, associated with in-plane THz phonon contribution. This band was sensitive to the phospholipid phase state that hints at its applicability for the phase coexistence problem in multicomponent lipid membranes. The low-frequency Raman spectroscopy of phospholipid bilayers is a very new method, and there are several issues to consider. How does the low-frequency Raman spectrum depend on the membrane composition? Does lateral or conformational ordering define the low-frequency spectral shape? Do embedded molecules (e.g., cholesterol) contribute to the low-frequency spectrum of the phospholipid bilayer? Can the low-frequency Raman spectrum distinguish between the case of the domain coexistence and a mixture of clusters homogeneous at a nanometer scale? These problems are addressed in the present study.

Low-frequency Raman scattering at room temperature was studied in three binary mixtures: fully saturated phospholipid (1,2-dipalmitoyl-sn-glycero-3-phosphocholine, DPPC) and cholesterol (Chol), doubly-unsaturated phospholipid (1,2-dioleoyl-sn-glycero-3-phosphocholine, DOPC) and cholesterol, and DPPC-DOPC. The DPPC-DOPC mixtures are known for the two-phase coexistence (Ref. [39] and references therein). There are no reports about the coexistence in the case of the DOPC-Chol mixture, while there are different views about the phase coexistence in the DPPC-Chol mixtures [19]. Also, these mixtures represent different phase states of phospholipid bilayers: solid-ordered (So, gel) in the case of DPPC, liquid-disordered (Ld, fluid) in the case of DOPC, and liquid-ordered (Lo, ordered hydrocarbon chains having high lateral and rotational mobility) attributed to the DPPC-Chol and DOPC-Chol compositions [19]. Thus, these binary mixtures allowed us to study the dynamic response on a nanometer scale in interesting cases by applying low-frequency Raman spectroscopy.

II. MATERIALS AND METHODS

A. Sample preparation

Saturated phospholipid DPPC and doubly-unsaturated phospholipid DOPC were purchased from Avanti Polar Lipids. Cholesterol was purchased from Sigma Aldrich. The substances were taken in different proportions, mixed, and dissolved in chloroform to prepare binary mixtures. Chloroform was vaporized from the mixtures by placing them under vacuum overnight. Then the mixtures were hydrated at 70 °C in the water excess condition, subjected to five freezing-thawing cycles (from liquid nitrogen temperature to 70 °C), and the excess water was removed by centrifugation. The final water-to-lipid weight ratio was typically in the range of 2–5. This sample preparation provides the aqueous suspensions of spherical multilamellar bilayers with typical diameters in the range of 1–10 μm. The suspensions were placed in glass tubes and hermetically sealed. The composition of the mixtures was verified by Raman spectroscopy. Deviations from the required compositions did not exceed 5%.

B. Raman experiment

A room-temperature (297 K) Raman scattering experiment was carried out with a triple-grating TriVista 777 spectrometer and a 532-nm solid-state laser. Right-angle light scattering was recorded with focusing and collecting lenses of 60-mm focal length. The spectral resolution was about 1 cm^{-1}. Raman spectra from ~5 to 800 cm^{-1} were recorded, using three spectral ranges as described in detail in Ref. [36].

Experimental spectra were corrected for a photoluminescence background and a bulk water contribution. Photoluminescence correction was done in a linear approximation, using two spectral areas, near 330 and 650 cm^{-1}, where Raman contributions from phospholipids and cholesterol are negligible [38]. In the previous work [38], the water contribution correction used the OH stretching band for normalization of the unpolarized Raman spectrum of water. In realization with the Raman setup with short spectral ranges, this way is very time consuming to achieve the high precision. Here, we applied another method. We used the observation that the Raman susceptibility of bulk water has a strong slope in the range from 200 to 300 cm^{-1}, while the lipid contribution is low and quasi-frequency-independent [38]. Thus, in the present work, we used this criterion for the water contribution correction. We checked for few samples that both methods are in good agreement.

Raman susceptibility $I_R(\omega)$ was found from the experimental Raman spectrum $I(\omega)$ via

$$I_R(\omega) = \frac{I(\omega)}{n(T,\omega)+1}, \tag{1}$$

where $n(T,\omega)$ is the Bose factor. Also, the spectra were normalized by the Raman intensity of the C–N mode (near 720 cm^{-1}) that intensity is believed to be phase independent [40].

III. RESULTS

Raman susceptibility spectra, evaluated from experimental spectra via Eq. (1) after the photoluminescence and water contribution corrections, are shown in Fig. 1 for the representative binary mixtures in the DOPC-DPPC series. Curves in Fig. 1 are normalized to the amplitude of the C-N stretching peak near 720 cm^{-1}.

Low-frequency Raman susceptibility of the phospholipid bilayers demonstrates a broad peak that has been attributed to the manifestation of the acoustic vibrational density of states [38]. The spectral shape and frequency of the maximum of this peak are different for the solid-ordered (gel) phase of pure DPPC and the liquid-disordered (fluid) phase of pure DOPC.

An interesting feature of the low-frequency Raman susceptibility is the narrow peak with a maximum near 7–11 cm^{-1}. This peak is too narrow to be a relaxation peak; thus, it reflects some vibrational motions. This peak is absent in the spectrum

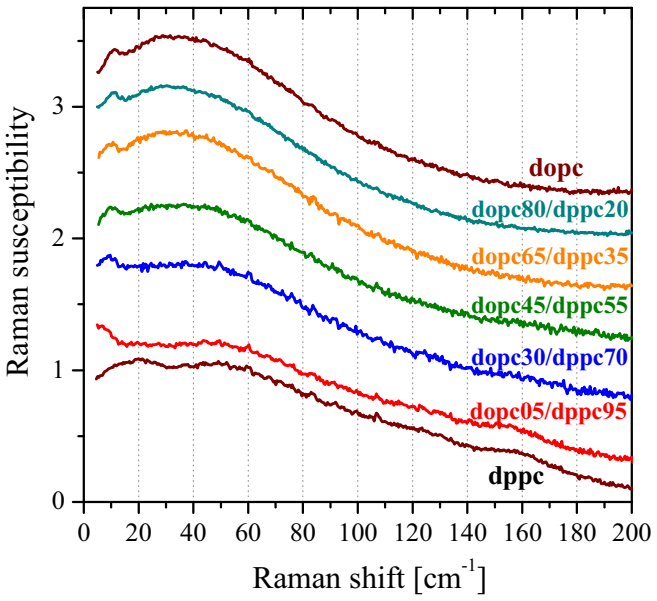

FIG. 1. Raman susceptibility spectra for various DOPC-DPPC mixtures. The spectra are normalized to the amplitude of the C-N stretching peak near 720 cm^{-1}. The spectra are vertically shifted for clarity.

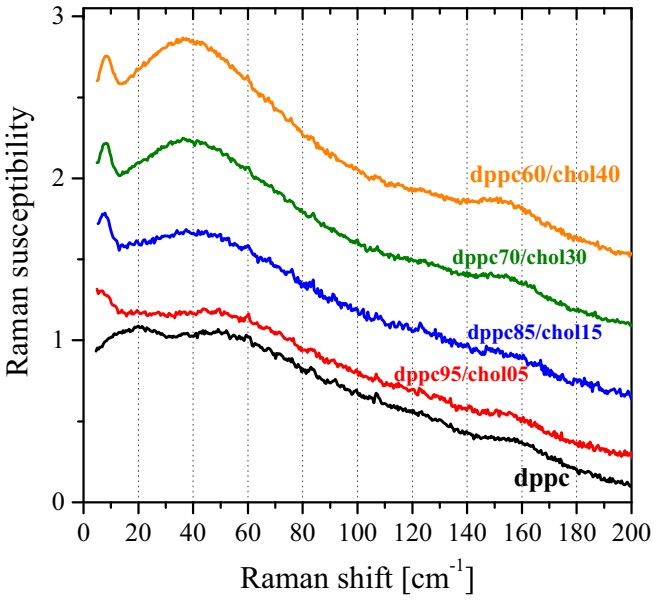

FIG. 2. Raman susceptibility spectra for various DPPC-Chol mixtures. The spectra are normalized to the amplitude of the C-N stretching peak near 720 cm^{-1}. The spectra are vertically shifted for clarity.

of pure DPPC sample but is manifested in the spectrum of the DOPC-DPPC mixture with 95 mol % of DPPC. In an analogy with the analysis of layer vibrational modes [35], this peak can be tentatively attributed to the monolayer vibrational eigenmode, which is absent in the case of strong elastic interaction between two leaflets of the phospholipid bilayer. (In this case, such vibrational motion corresponds to the second eigenmode of bilayer and is forbidden for Raman scattering). Thus, the role of 5 mol % is to break the coherence of the vibrational motions in two leaflets of the phospholipid bilayer. For the rest of the paper, we will use the term "layer mode" for this eigenmode. If the layer mode also has a nonzero wave-vector component along the phospholipid layer, it will correspond to the term "transversal mode" from the viewpoint of INS or IXS.

Figure 1 shows that the low-frequency Raman susceptibility is very similar for the DOPC-DPPC mixtures with the DPPC fraction less than 40 mol %. These mixtures represent the liquid-disordered phase according to the phase diagram [39]. For the DPPC fractions between 40 and 95 mol %, the spectral shape of the susceptibility continuously changes.

Raman susceptibility spectra of the binary mixtures in the DPPC-Chol series are shown in Fig. 2. Qualitatively the effect of the cholesterol addition is similar as in Fig. 1. Already 5 mol % of cholesterol significantly changes the spectrum of pure DPPC below 30 cm^{-1}. The spectra for the cholesterol concentration between 30 and 40 mol % are very similar, while they continuously evaluate for the Chol concentration between 5 and 30 mol %.

It is generally believed that the high concentration of cholesterol in saturated phospholipids leads to the liquid-ordered phase [19]. Comparison of Figs. 1 and 2 allows one to conclude that the low-frequency Raman susceptibility of the liquid-ordered phase is similar to one of the liquid-disordered phase. Thus, we can conclude that lateral ordering and mobility play a crucial role in the low-frequency Raman susceptibility spectral shape.

An interesting detail in Fig. 2 is a bump near 157 cm^{-1} in the spectrum of DPPC, which corresponds to the longitudinal acoustic mode (accordion-like mode) [41,42]. The apparent intensity of this mode increased with cholesterol, but this is due to the contribution of an intramolecular mode of cholesterol, which is near 150 cm^{-1}.

Raman susceptibility spectra of the binary mixtures in the DOPC-Chol series are shown in Fig. 3. It is usually believed that the cholesterol addition to the unsaturated DOPC leads to the liquid-ordered phase [19]. It is seen that qualitatively the low-frequency Raman susceptibility of various compositions in the DOPC-Chol series is very similar, regardless of the supposed difference in the conformational state.

The broad peak in the Raman susceptibility (Figs. 1–3) is explained by the contribution of the acoustic vibrational density of states due to disorder-induced breaking of the scattering wave-vector limitation. It is interesting to compare the band intensity for different phospholipid bilayer phases. Two parameters were evaluated from the experimental spectra: amplitude of the broad peak and the integral from the lowest frequency to 200 cm^{-1}. Both parameters are shown in Fig. 4 for three binary series. It is seen that the lowest value is observed for the compositions with the presence of the gel (solid-ordered) phase. Lateral disordering leads to an increase in the broad peak amplitude (Fig. 4 bottom), while it is less significant in the case of the integral (Fig. 4 top). In general, the broad peak in the DOPC-DPPC series is of the same order of amplitude. Therefore, while, generally, the So phase is more ordered in the lateral plane, lack of the long-range order is responsible for the broad peak intensity on a similar level as for the Ld phase.

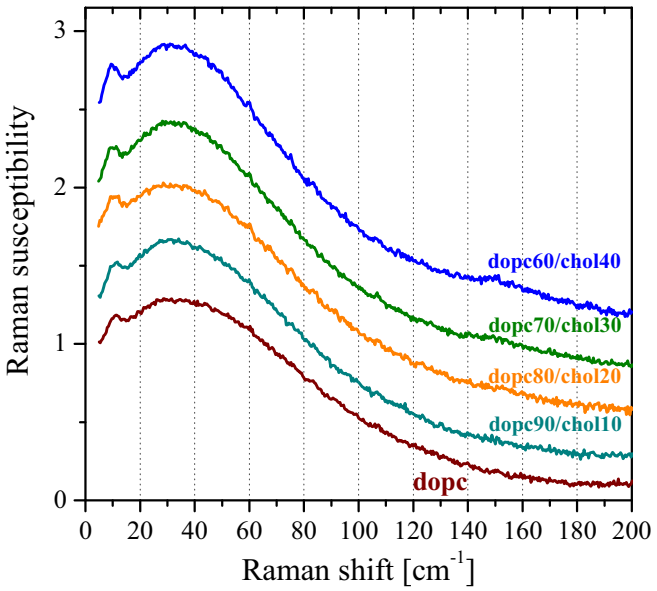

FIG. 3. Raman susceptibility spectra for various DOPC-Chol mixtures. The spectra are normalized to the amplitude of the C-N stretching peak near 720 cm^{-1}. The spectra are vertically shifted for clarity.

The cholesterol addition increases the broad peak intensity, as is seen in Fig. 4. This can be explained by the contribution of cholesterol molecules into the acoustic motion manifested in the low-frequency Raman spectrum (CN mode used for the spectral normalization belongs solely to the phospholipid spectrum).

In search of simple parameters of low-frequency Raman susceptibility, which could distinguish different phases of phospholipid bilayers, we addressed the position of the maximum and width for the broad peak. For this purpose, the experimental susceptibility was fitted by a quadratic polynomial near the maximum (for the experimental points above

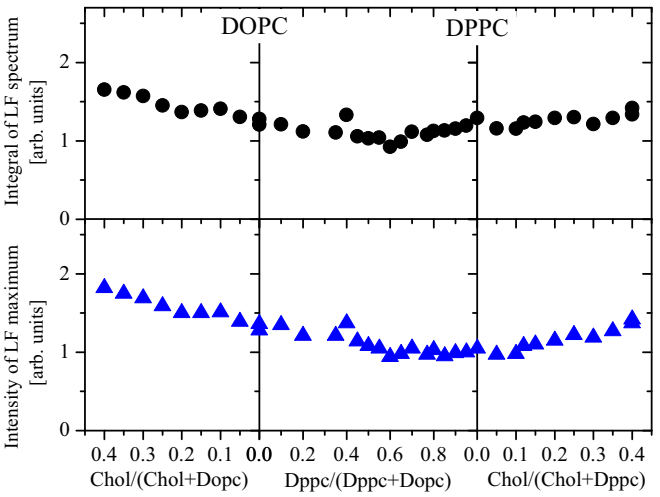

FIG. 4. Amplitude of the broad peak in the low-frequency Raman susceptibility (bottom) and its integral over 5–200 cm^{-1} (top) versus the compositions of the binary phospholipid-phospholipid and phospholipid-cholesterol series.

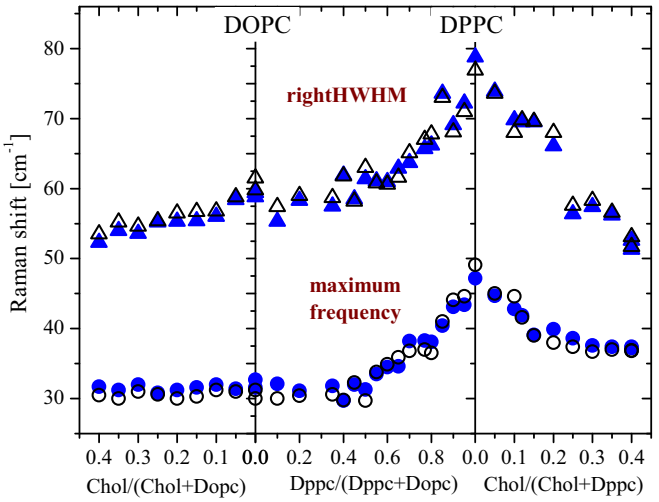

FIG. 5. Frequency of the maximum (circles) and right HWHM (triangles) of the broad peak in the low-frequency Raman susceptibility versus the binary composition. The open symbols correspond to the evaluation implying the smoothing, and the solid symbols to a quadratic polynomial fitting near the maximum.

0.9 level of the intensity of the maximum). Right half-width at half-maximum (HWHM) was determined as the difference between the spectral positions of the half-intensity and the maximum. Alternatively, the frequency of the maximum and right HWHM were found as apparent parameters after smoothing (adjacent-averaging) of the experimental spectra. The broad peak parameters are shown in Fig. 5 for three binary series. Good agreement between the two ways of parameter estimation confirms the evaluation.

It can be seen that the right HWHM reflects the differences in the spectral shapes of solidlike and liquid (Ld or Lo) phases of phospholipid bilayers. It is significantly higher for the compositions with gel phase contribution, reflecting smoother cut-off of the vibrational density of states. For the compositions, where liquid (Ld or Lo) phases dominate, the right HWHM parameter is approximately the same. Also, the position of the maximum reflects the phase state of phospholipid bilayers. It is higher for compositions with a high fraction of the solidlike phase. This corresponds to the higher sound velocities (and, therefore, stiffness) in these compositions.

While usually the phase state of DOPC-Chol and DPPC-Chol with the high cholesterol concentration is described similarly as liquid-ordered, the frequency of the maximum clearly distinguishes these cases. The position of the maximum is higher in the DPPC-Chol case in comparison with the case of DOPC-Chol. We attribute this to the difference in the conformational ordering of saturated and unsaturated phospholipids. Conformational ordering increases the bilayer stiffness, in other words, the sound velocity, and, therefore, the phonon frequency at the same wave vector. This is the reason for the higher frequency of the maximum in the vibrational density of states. It seems the cholesterol-induced conformational ordering is low (if any) in the case of DOPC, while a significant part of DPPC molecules rests in the all-trans-conformational states. The difference in the bump near 150–160 cm^{-1}, in which the all-trans mode and cholesterol

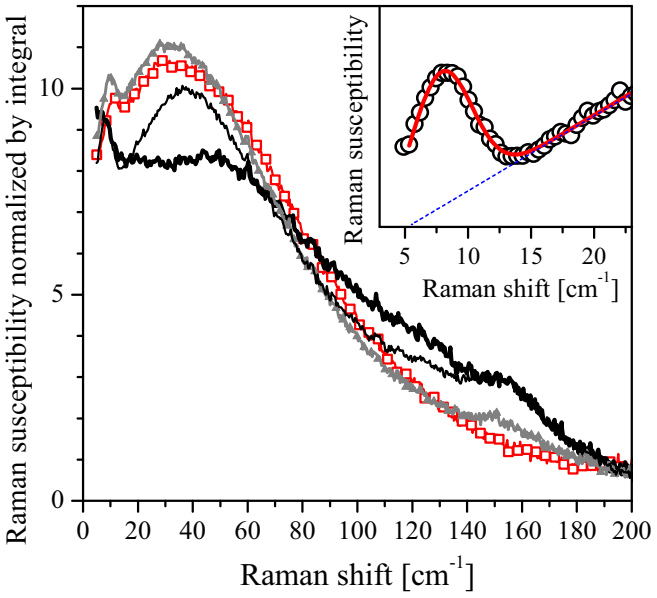

FIG. 6. Raman susceptibility spectra for the So phase (DPPC95-Chol05 mixture, thick line), the Ld phase (DOPC, squares), liquidlike phase of DOPC60-Chol40 (gray line), and Lo phase of DPPC60-Chol40 (thin line). The inset shows the low-frequency part of the DPPC60-Chol40 spectrum (circles) with the linear extrapolation of the broad peak contribution (dotted line) and Gaussian description of the layer mode (solid line).

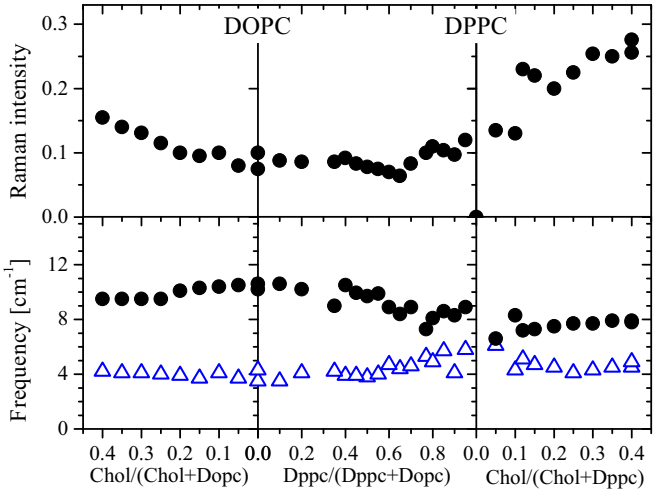

FIG. 7. Amplitude (top), position of the maximum (bottom, circles), and width (bottom, triangles) of the layer mode versus the binary composition.

mode contribute, for the DPPC-Chol and DOPC-Chol mixtures with the same cholesterol fraction, supports this view. Thus the frequency of the maximum fairly distinguishes the liquid-ordered (DPPC-Chol) and liquid-disordered (DOPC, DOPC-Chol) phases.

Figure 6 compares the spectral shape of different phospholipid phases. Normalization of the spectra by the integral over the low-frequency Raman susceptibility is used in this figure. Also, to avoid peculiarities of the pure DPPC, the spectrum for the DPPC-Chol mixture with 5 mol % of Chol is shown as a representative for the So phase. It is seen that the Raman spectrum allows one to determine whether phospholipid bilayers are in the So phase or liquid (Ld or Lo) phases.

The inset of Fig. 6 presents the spectral part of the Raman susceptibility near the layer mode. Description of the layer mode with a Gaussian approximation and a linear extrapolation of the broad peak spectrum are shown in this inset. We used this way to quantify the composition dependence of the layer mode. Parameters of Gaussian fitting of the layer mode are shown in Fig. 7.

The amplitude of the layer mode is zero for pure DPPC, but already addition of a small (5 mol %) amount of DOPC or Chol leads to the appearance of the layer mode in the spectra. This is in line with the view that this line is absent in the DPPC spectrum only due to the symmetry reason. The amplitude is lowest for the DOPC-DPPC mixture (probably with an increase in the range of 65–95 mol % of DPPC). The intensity of the layer mode increases with the cholesterol concentration. Considering the normalization to the CN mode Raman intensity, this is in favor that cholesterol molecules are involved in the vibrational motion, as it should be expected for the collective layer mode. A striking observation is that the cholesterol effect on the layer mode intensity is higher in the DPPC-Chol mixture. The reason for this is not clear, but ambiguities in the linear extrapolation of the broad peak cannot be excluded. Further investigations are needed to clarify this point. The typical width of the layer mode was 4–5 cm^{-1} without a pronounced composition dependence.

The frequency of the layer mode was 7–8 cm^{-1} in the mixtures with the high concentration of DPPC and 10–11 cm^{-1} for the high concentration of DOPC (Fig. 7). The frequency of the layer eigenmode, involving the layer thickness fluctuation, is expected to be determined by the ratio of the sound velocity and thickness [34]. The Ld phase has a lower sound velocity and a smaller thickness compared to ordered phases. It seems that the relative decrease of the thickness in the Ld phases is higher than the decrease in the sound velocities. This case leads to higher layer frequency in the Ld phase. The layer mode seems to distinguish the conformationally ordered and disordered phases (Fig. 7).

Figures 5–7 demonstrate the potential of the low-frequency Raman susceptibility in the identification of the lipid phase states. But what is the capability of the dynamic response on a nanometer scale for the homogeneity characterization of multicomponent lipid bilayers? These bilayers can be homogeneous on the nanometer scale or consist of well-defined domains of coexisting phases. In the case of the coexistence, the Raman spectrum of a lipid mixture must be the sum of the spectra of compositions, corresponding to boundaries of the coexistence range. The contribution of these spectra to the sum should be defined by the lever rule [19]. It is convenient to analyze this problem with the difference spectrum, as it is done below.

Low-frequency Raman susceptibility spectra in the DOPC-DPPC mixtures normalized by their integral are shown in Fig. 8(a). Here, the DOPC-DPPC mixture with 5 mol % represents the gel phase to avoid problems of the peculiarity of pure DPPC. The isosbestic point near 83 cm^{-1} [Fig. 8(a)] is a reliable indicator of the superposition of Raman spectra of

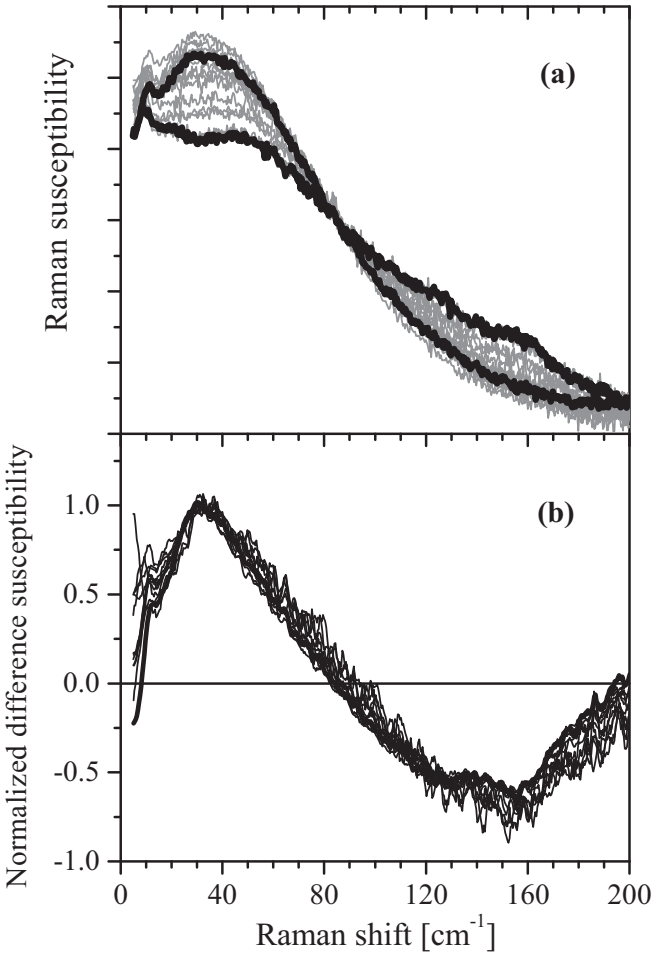

FIG. 8. (a) Raman susceptibility spectra for the DOPC-DPPC mixtures. The thick lines are DOPC and the mixture with 5 mol % of DOPC. The gray lines show the spectra for the mixtures with 10, 15, 20, 23, 30, 35, 40, 45, 50, 55, 65, 80, 90 mol % of DOPC. (b) Difference spectra between a particular spectrum and one of the mixture with 5 mol % of DOPC, the difference spectra were normalized to its amplitude. The thick line is the difference spectrum for DOPC, and the gray lines are for the mixtures with 20, 23, 30, 35, 40, 45, 50, 55, 65, 80, 90 mol % of DOPC.

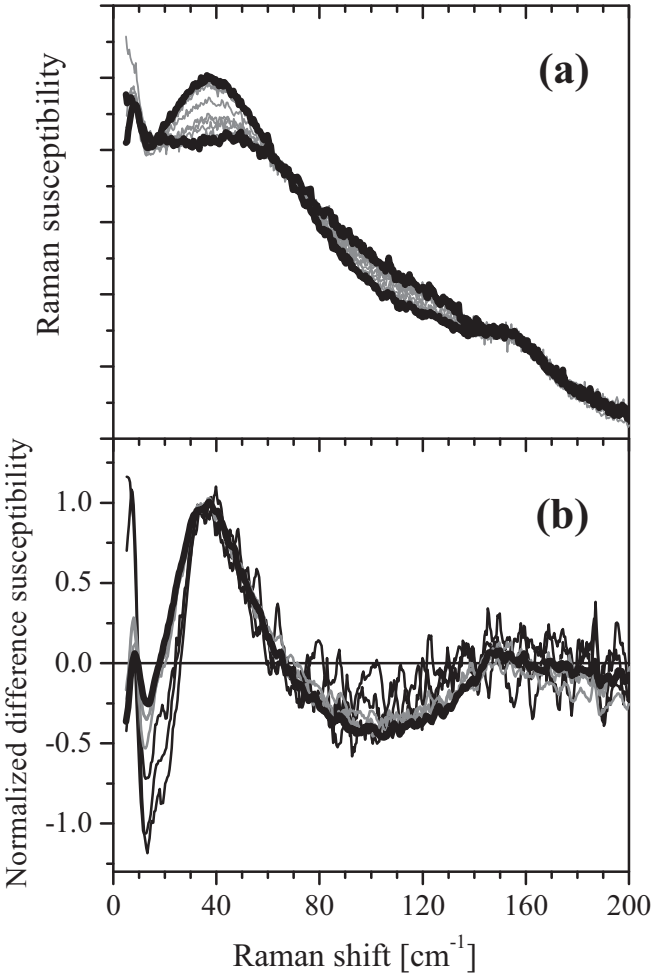

FIG. 9. (a) Raman susceptibility spectra for the DPPC-Chol mixtures. The thick lines correspond to the mixtures with 5 and 40 mol % of Chol. The gray lines show the spectra for the mixtures with 10, 12, 15, 20, 25, 30, 35 mol % of Chol. (b) Difference spectra between a particular spectrum and one of the mixture with 5 mol % of Chol, the difference spectra were normalized to its amplitude. The thin lines are the difference spectrum for the mixtures with 12, 15, 20 mol % of Chol, the gray lines for the mixtures with 25, 30, 35 mol % of Chol, the thick solid line corresponds to the mixture with 40 mol % of Chol.

two species. If any spectrum is a superposition of two spectra corresponding to the gel and liquid-disordered phases, the difference between the superposition and the spectrum of the gel phase must have the same spectral shape. We found such difference spectra and normalized them by their amplitude to test this expectation. Results are shown in Fig. 8(b) for all compositions of the DOPC-DPPC mixture, except for 10 and 15 mol %, which appear to be noisier and have been omitted for illustrative purposes. It can be seen that the difference spectra demonstrate the same spectral shape in the range of 14–200 cm^{-1}. This validates that any spectrum of the DOPC-DPPC mixtures is the superposition of Raman spectra of the gel and liquid-disordered phases.

The superposition assumption works worse for the Raman shift below ∼10 cm^{-1}. The range below 10 cm^{-1} is close to the spectral boundary and also includes the relaxation response. At present, it is difficult to judge the origin of the master plot violation below 10 cm^{-1}. Probably, the relaxation response sensitive to defect structure does not follow the superposition rule.

A similar analysis of the superposition rule for the low-frequency Raman susceptibility was done for the DPPC-Chol mixtures. Results are shown in Fig. 9. The isosbestic point, which is seen in Fig. 9(a), indicates the superposition rule. Indeed, the difference spectra in Fig. 9(b) confirm the fairness of the superposition in the range above ∼30 cm^{-1}, near the maximum and for higher frequencies. It is expected that the vibrational density of states near the maximum reflects the properties of the phonons with wavelengths slightly higher than the neighbor molecule distance [38]. Thus, the results of Fig. 9 agree with the coexistence of two kinds of clusters of DPPC and cholesterol on the neighbor molecule scale.

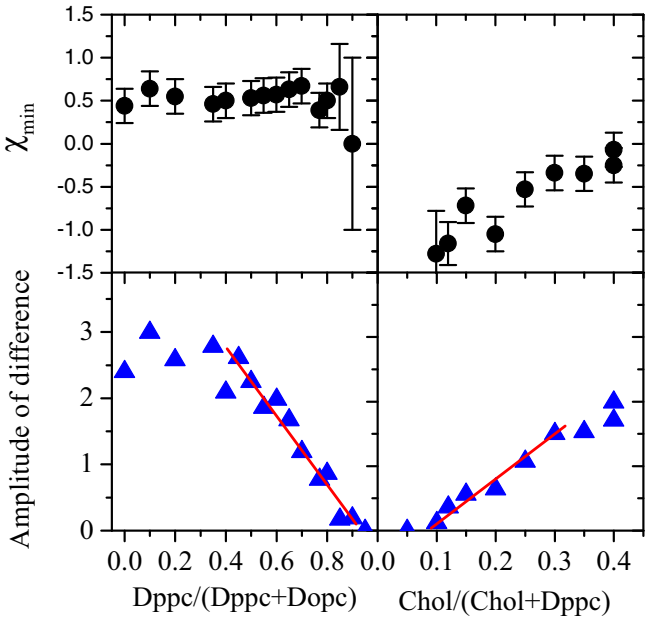

FIG. 10. (Top) Raman susceptibility at minimum in the normalized difference spectra of Figs. 8 and 9 versus the binary composition. (Bottom) The amplitude of the difference spectra used for the normalization in Figs. 8 and 9 (triangles) versus the binary composition. The lines describe the composition dependences in the supposed coexistence range.

On the other hand, the spectral shape for the difference spectra below 30 cm^{-1} varies significantly for the DPPC-Chol mixtures. It is important that the superposition breaks for the composition range of 12–25 mol % of Chol, where the domain coexistence is expected, according to some previous works. The boundaries of the coexistence range differ slightly in different works (see, Ref. [43] for review).

We tested whether the difference spectra in Figs. 8 and 9 have the amplitudes consistent with the lever rule in the coexistence ranges. The amplitudes used for normalization in Figs. 8 and 9 are shown in Fig. 10 bottom versus the binary composition. It can be seen that in the coexistence ranges (40–95 mol % of DPPC in the case of DOPC-DPPC mixtures and 10–30 mol % of Chol in DPPC-Chol mixtures), the linear dependences work well. Outside of these ranges, the amplitudes can be described as constants. Thus, the amplitudes of the difference spectra are consistent with the lever rule in the coexistence ranges.

We quantified the apparent deviations below 30 cm^{-1} from the master curve of the difference spectra in the case of DPPC-Chol mixtures. The most deviation is seen at the minimum between the maxima near 40 and 10 cm^{-1} (Fig. 9). In Fig. 10 top, the value of the minimum in the difference spectra is shown versus the DPPC-Chol composition. For comparison, the value of the similar minimum in the DOPC-DPPC mixture is also shown in Fig. 10. It is seen that the minimum is composition independent in the DOPC-DPPC mixtures but changes monotonously in the coexistence range of the DPPC-Chol mixtures. Thus the low-frequency Raman response contradicts the hypothesis of coexisting domains with size above several nanometers in the DPPC-Chol mixtures.

Low-frequency Raman susceptibility is very similar in the DOPC-Chol mixtures (Figs. 3 and 6). So, the analysis of the difference spectra was not carried out for these mixtures.

IV. DISCUSSION

Low-frequency Raman susceptibility spectra of three series of binary lipid mixtures were studied. The broad peak with the maximum in the range of 30–50 cm^{-1}, having the same order of intensity, was observed for all compositions. Thus, this broad peak is the universal feature of the Raman susceptibility in lipid bilayers. To the best of our knowledge, except in the previous work [38], this spectral range in Raman scattering of lipid bilayers was not studied before at physiological temperatures. Comparison with the phonon dispersion relations, done in Ref. [38] for available INX and INS data, favors that the broad peak reflects the lateral phonon density of states. Here, we found that the cholesterol addition increases the broad peak intensity (Fig. 4), confirming the collective character of vibrational excitations, which contributes to this band. It would be interesting to evaluate the so-called Raman coupling coefficient, which relates the vibrational density of states with the low-frequency Raman spectrum [44]. Frequency dependence of the coupling coefficient would clarify the description of the THz phonons in phospholipid bilayers. Unfortunately, to the best of our knowledge, the vibrational density of states has not yet been measured in phospholipid bilayers using the INS or IXS techniques. In general, the manifestation of dynamic response on a nanometer scale in the low-frequency Raman scattering of lipid bilayers can become an interesting new field in physics and chemistry of lipids.

Except for the pure So (gel) state, all other compositions showed a narrow peak in the susceptibility spectrum in the range of 7–11 cm^{-1}. The increase of the peak amplitude with the cholesterol addition (Fig. 7) means the collective character of this vibrational mode. Here, this mode is referred to as the "layer mode", reflecting the thickness change during this vibration (the term "thickness breathing mode" is used for the similar mode in the Raman spectrum of nanometer-thin semiconductor platelets [45]). Adding the nonzero phonon wave vector in the lateral plane turns this mode into a kind of transversal mode with an off-plane displacement. Recently, analysis of IXS data revealed a transversal mode near 1 meV (8 cm^{-1}) for a phospholipid-cholesterol mixture [32]. In this work, the frequency of the transversal mode had a very low wave-vector dependency in the range of 1–10 nm^{-1} that has to result in a narrow peak for the vibrational density of states. So, it looks likely that the layer peak in Raman scattering reflects the density of transversal phonon states. In Ref. [46], this transversal phonon was described as a shear mode with displacements in the lateral plane. Thus, the considered possibilities agree that the layer peak corresponds to vibrations with transversal displacements relative to the wave vector, but further investigations are needed to clarify whether these modes are thickness breathing or shear.

The high spectral resolution of the Raman experiment reveals the composition dependence of the layer peak in detail (Fig. 7). It seems that its frequency is more sensitive to the conformational ordering (see the DPPC-Chol mixture data in Fig. 7) than to the lateral one.

Composition dependence of the broad peak parameters revealed that the spectral shape is mostly influenced by the lateral order as it can be seen in Fig. 6 and was quantified by the right HWHM in Fig. 5. Liquid (Ld or Lo) phases demonstrated a more Gaussian-like spectral shape than the So phase, where the band has a flatlike shape up to $\sim$50 cm^{-1} and smoother descent at higher frequencies.

Figure 5 provides evidence that even the position of the maximum can be helpful in identifying the phase state of lipid bilayers. In the description of this figure, we have taken into account that while the DOPC-Chol mixture with high cholesterol concentration is described as the liquid-ordered phase [19], there is no evidence of significant cholesterol-induced conformational ordering DOPC hydrocarbon chains, to the best of our knowledge. In this sense, the DOPC-Chol mixtures can be considered as being in the liquid-disordered phase. The frequency of the maximum is near 30 cm^{-1} for Ld phase and close to 48 cm^{-1} for So phase. The higher position of the maximum should be related to higher stiffness (sound velocity) for higher conformational and lateral ordering. An interesting case is DPPC-Chol mixtures with high cholesterol concentrations. These mixtures have high conformational ordering but liquidlike lateral ordering. The position of the maximum is near 37 cm^{-1}, being intermediate between ones of the So and Ld phases. The results of Fig. 5 mean that both conformational and lateral orderings are important for the position of the maximum of the broad peak.

Composition dependence of the broad peak parameters in the case of DOPC-DPPC and DPPC-Chol mixture in Fig. 5 hints at the possibility of coexisting phases. Analysis, which was carried out in Figs. 8 and 10, proves the coexisting domains of So and Ld phases in DOPC-DPPC mixtures for the DPPC concentration from 40 to 95 mol %.

A similar analysis in the DPPC-Chol mixtures confirms the fidelity of the superposition rule for the Raman shift above 30 cm^{-1} (Figs. 9 and 10). The violation from the master curve for the difference spectra below 30 cm^{-1} (Fig. 9) contradicts the assumption about the coexistence of the phase domains with size significantly above neighbor molecule distance. Considering typical longitudinal sound velocity of about 2 km/s for phospholipid bilayers at temperatures slightly below the So-Ld (gel-fluid) transition [47], a frequency of 30 cm^{-1} corresponds to acoustic waves with a wavelength of 2 nm. Therefore, the results of the present study evidence that on the scale of several nanometers and above, there are no coexisting domains of well-defined phases in the DPPC-Chol mixtures. On the other hand, the difference spectra are consistent with the coexistence of two kinds of clusters at the scale of neighbor molecules. So, cholesterol forms the phospholipid-cholesterol complexes (clusters) with a homogeneous spatial distribution on the scale above several nanometers. Some previous works [48–50] used the formation of phospholipid-cholesterol complexes to describe experimental results in saturated phospholipid-cholesterol mixtures. Low-frequency Raman spectroscopy supports this view but points to the homogeneous distribution of clusters in bilayers. Possible images of phospholipid-cholesterol clusters were presented in simulation studies (e.g., Refs. [51,52]).

An important peculiarity of the low-frequency Raman spectra found in the present work is its sensitivity to lateral ordering. Such property is scarce for molecular Raman spectroscopy in phospholipid bilayers, which is usually sensitive to the conformational states of molecules.

V. CONCLUSIONS

The dynamic response on a nanometer scale of aqueous solutions of vesicles from binary mixtures of saturated/unsaturated phospholipids, saturated phospholipid/cholesterol, and unsaturated phospholipid/cholesterol was studied with low-frequency Raman spectroscopy. Different binary series represented different scenarios for possible phase coexistence: without the phase coexistence, the coexistence of liquid-disordered and solidlike phases, and the coexistence of solid-ordered and liquid-ordered phases. It was established that the low-frequency Raman susceptibility of all compositions includes a broad peak, reflecting the acoustic vibrational density of states. This band differs for different lipid phases and distinguishes liquid (Ld or Lo) and So lateral ordering. Also, a narrow peak attributed to layer modes was found for all compositions, except the saturated phospholipid in the So phase. Parameters of this peak were sensitive to the conformational order of hydrocarbon chains. These results make the low-frequency Raman spectroscopy an excellent tool for studying the phase states and the dynamic response on a nanometer scale in lipid bilayers.

It was shown that the low-frequency Raman susceptibility reveals the phase coexistence on a nanometer scale in lipid bilayers and distinguishes the case of homogeneous distribution of molecular complexes (saturated phospholipid/cholesterol mixtures) from coexisting domains with size above several nanometers (saturated phospholipid/unsaturated phospholipid mixtures).

ACKNOWLEDGMENTS

This work was supported by Russian Science Foundation, Grant No. 19-12-00127. Some part of the experiments was performed in the multiple-access center "High-Resolution Spectroscopy of Gases and Condensed Matter" in IA&E SBRAS (Novosibirsk, Russia).

[1] M. C. Wiener and S. H. White, Biophys. J. **61**, 434 (1992).
[2] K. Akabori and J. F. Nagle, Soft Matter **11**, 918 (2015).
[3] J. F. Nagle, P. Cognet, F. G. Dupuy, and S. Tristram-Nagle, Chem. Phys. Lipids **218**, 168 (2019).
[4] D. Marquardt, F. A. Heberle, J. Pan, X. Cheng, G. Pabst, T. A. Harroun, N. Kucerka, and J. Katsaras, Chem. Phys. Lipids **229**, 104892 (2020).
[5] J. J. Kinnun, H. L. Scott, R. Ashkar, and J. Katsaras, Front. Chem. **9**, 203 (2021).
[6] J. L. Thewalt and M. Bloom, Biophys. J. **63**, 1176 (1992).
[7] H. I. Petrache, S. W. Dodd, and M. F. Brown, Biophys. J. **79**, 3172 (2000).
[8] T. Yasuda, H. Tsuchikawa, M. Murata, and N. Matsumori, Biophys. J. **108**, 2502 (2015).

[9] M. J. Swamy, L. Ciani, M. Ge, A. K. Smith, D. Holowka, B. Baird, and J. H. Freed, Biophys. J. **90**, 4452 (2006).

[10] S. A. Dzuba, E. P. Kirilina, and E. S. Salnikov, J. Chem. Phys. **125**, 054502 (2006).

[11] P. Sassi, S. Caponi, M. Ricci, A. Morresi, H. Oldenhof, W. F. Wolkers, and D. Fioretto, and J. Raman Spectrosc. **46**, 644 (2015).

[12] K. Czamara, K. Majzner, M. Z. Pacia, K. Kochan, A. Kaczor, and M. Baranska, J. Raman Spectrosc. **46**, 4 (2015).

[13] A. A. Dmitriev and N. V. Surovtsev, J. Phys. Chem. B **119**, 15613 (2015).

[14] J. R. Silvius, D. del Giudice, and M. Lafleur, Biochem. **35**, 15198 (1996).

[15] S. Donaldson and H. B. de Aguiar, J. Phys. Chem. Lett. **9**, 1528 (2018).

[16] S. L. Veatch and S. L. Keller, Biochim. Biophys. Acta **1746**, 172 (2005).

[17] J. Juhasz, F. J. Sharom, and J. H. Davis, Biochim. Biophys. Acta **1788**, 2541 (2009).

[18] K. Simons and E. Ikonen, Nature (London) **387**, 569 (1997).

[19] D. Marsh, Biochim. Biophys. Acta **1788**, 2114 (2009).

[20] N. Kumar, M. M. Drozdz, H. Jiang, D. M. Santos, and D. J. Vaux, Chem. Commun. **53**, 2451 (2017).

[21] M. A. Alonso and J. Millán, J. Cell Sci. **114**, 3957 (2001).

[22] D. A. Brown and E. London, Annu. Rev. Cell Dev. Biol. **14**, 111 (1998).

[23] P. M. Winkler, R. Regmi, V. Flauraud, J. Brugger, H. Rigneault, J. Wenger, and M. F. Garcia-Parajo, J. Phys. Chem. Lett. **9**, 110 (2017).

[24] D. Lingwood and K. Simons, Science **327**, 46. (2010).

[25] S. Sonnino and A. Prinetti, Curr. Med. Chem. **20**, 4 (2013).

[26] E. Sezgin, I. Levental, S. Mayor, and C. Eggeling, Nat. Rev. Mol. Cell Biol. **18**, 361 (2017).

[27] S. H. Chen, C. Y. Liao, H. W. Huang, T. M. Weiss, M. C. Bellisent-Funel, and F. Sette, Phys. Rev. Lett. **86**, 740 (2001).

[28] M. C. Rheinstädter, C. Ollinger, G. Fragneto, F. Demmel, and T. Salditt, Phys. Rev. Lett. **93**, 108107 (2004).

[29] M. Zhernenkov, D. Bolmatov, D. Soloviov, K. Zhernenkov, B. P. Toperverg, A. Cunsolo, A. Bolsak, and Y. Q. Cai, Nat. Commun. **7**, 11575 (2016).

[30] C. L. Armstrong, M. A. Barrett, A. Hiess, T. Saldit, J. Katsaras, A. C. Shi, and M. C. Rheinstädter, Eur. Biophys. J. **41**, 901 (2012).

[31] G. D'Angelo, V. C. Nibali, U. Wanderlingh, C. Branca, A. De Francesco, F. Sacchetti, C. Petrillo, and A. Paciaroni, J. Phys. Chem. Lett. **9**, 4367 (2018).

[32] D. Bolmatov, D. Soloviov, M. Zhernenkov, D. Zav'yalov, E. Mamontov, A. Suvorov, Y. Q. Cai, and J. Katsaras, Langmuir **36**, 4887 (2020).

[33] J. Jackle, in *Amorphous Solids: Low-Temperature Properties*, edited by W. A. Phillips (Springer, Berlin, 1981), p. 135.

[34] N. V. Surovtsev, A. A. Dmitriev, and S. A. Dzuba, Phys. Rev. E **95**, 032412 (2017).

[35] A. A. Dmitriev, and N. V. Surovtsev, J. Raman Spectrosc. **50**, 1691 (2019).

[36] D. V. Leonov, S. V. Adichtchev, S. A. Dzuba, and N. V. Surovtsev, Phys. Rev. E **99**, 022417 (2019).

[37] D. V. Leonov, S. A. Dzuba, and N. V. Surovtsev, RSC Adv. **9**, 34451 (2019).

[38] N. V. Surovtsev and S. V. Adichtchev, J. Raman Spectrosc. **51**, 952 (2020).

[39] S. V. Adichtchev, K. A. Okotrub, A. M. Pugachev, I. V. Zaytseva, and N. V. Surovtsev, Appl. Spectrosc. **75**, 87 (2021).

[40] B. P. Gaber and W. L. Peticolas, Biochim. Biophys. Acta **465**, 260 (1977).

[41] A. Schaufele and T. Shimanouchi, J. Chem. Phys. **47**, 3605 (1967).

[42] D. F. Wallach, S. P. Verma, and J. Fookson, Biochim. Biophys. Acta **559**, 153 (1979).

[43] D. Marsh, Biochim. Biophys. Acta **1798**, 688 (2010).

[44] N. V. Surovtsev and A. P. Sokolov, Phys. Rev. B **66**, 054205 (2002).

[45] A. Girard, L. Saviot, S. Pedetti, M. D. Tessier, J. Margueritat, H. Gehan, B. Mahler, B. Dubertret, and A. Mermet, Nanoscale **8**, 13251 (2016).

[46] D. Bolmatov, J. J. Kinnun, J. Katsaras, and M. O. Lavrentovich, Chem. Phys. Lipids. **232**, 104979 (2020).

[47] V. A. Zykova, S. V. Adichtchev, and N. V. Surovtsev, J. Phys. Chem. B **124**, 9079 (2020).

[48] D. Needham, T. J. McIntosh, and E. Evans, Biochem. **27**, 4668 (1988).

[49] K. A. Okotrub, I. V. Zaytseva, S. V. Adichtchev, and N. V. Surovtsev, Biochim. Biophys. Acta **1863**, 183514 (2021).

[50] H. M. McConnell and A. Radhakrishnan, Biochim. Biophys. Acta **1610**, 159 (2003).

[51] S. W. Chiu, E. Jakobsson, R. J. Mashl, and H. L. Scott, Biophys. J. **83**, 1842 (2002).

[52] S. A. Pandit, D. Bostick, and M. L. Berkowitz, Biophys. J. **86**, 1345 (2004).